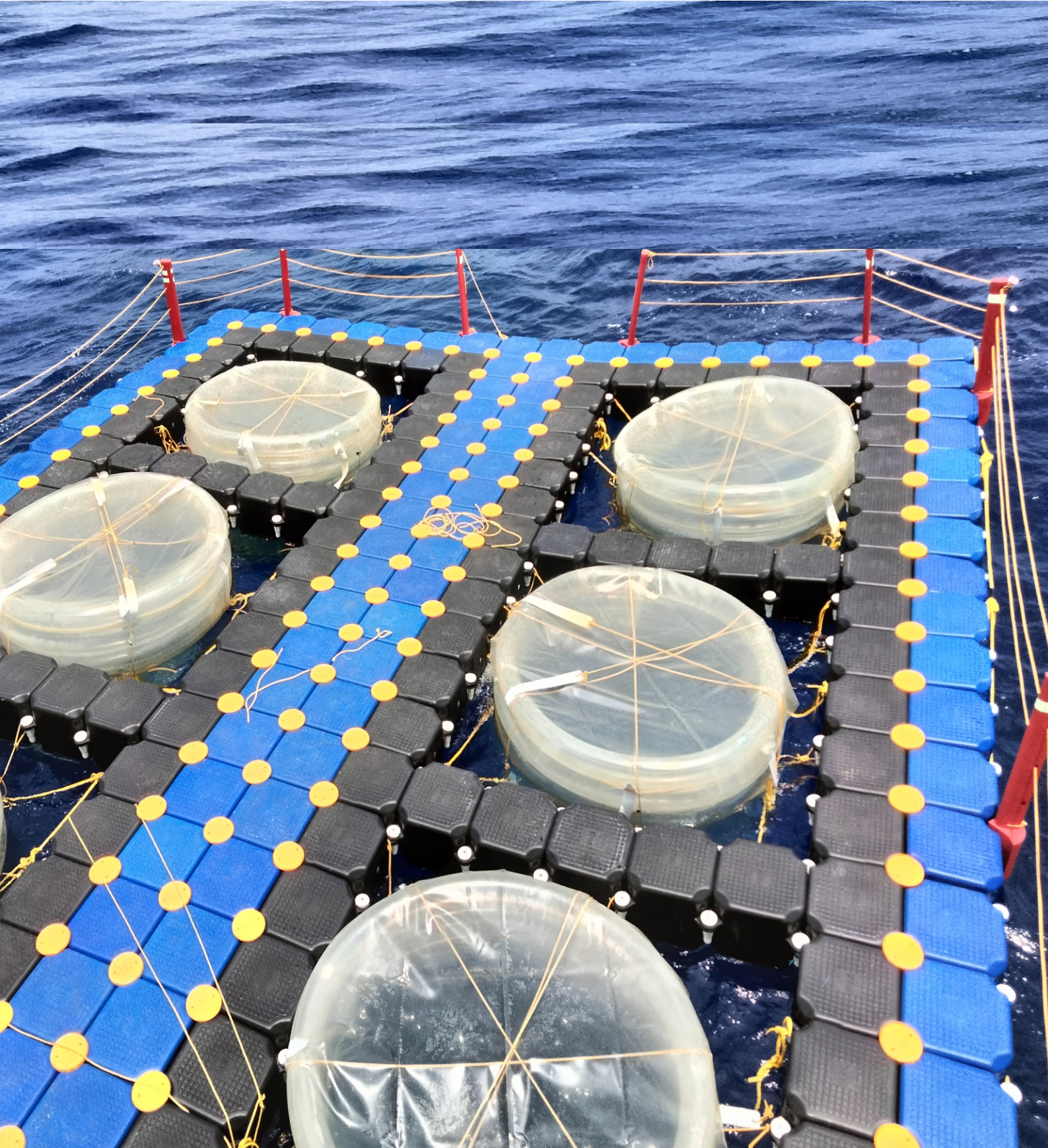


OCEAN DIGEST



Quarterly Newsletter of the Ocean Society of India

Volume 10 | Issue 1 | January 2023 | ISSN 2394-1928



Precipitation Isotope Statistics during Low-Pressure Systems and Cyclones: Implications for Paleo-monsoon Reconstruction



S. Chakraborty^{1*}, Amey Datye², Pramit K. Deb Burman³, M.G. Yadava⁴, P.M. Mohan⁵

¹Department of Atmospheric and Space Sciences, Savitribai Phule Pune University, Pune

²Indian Institute of Tropical Meteorology, Pune

³Center for Climate Change Research, Indian Institute of Tropical Meteorology, Pune

⁴Physical Research Laboratory, Ahmedabad

⁵Department of Ocean Studies and Marine Biology, Pondicherry University, Port Blair

* Author for correspondence; Email: supriyoc@gmail.com

Abstract

Precipitation isotope ratios can provide useful information about the moisture transport processes and the sources of water vapor in the atmosphere. Low-pressure systems (LPSs) and cyclones are essential features of the Indian monsoon that bring significant rainfall to the northern Indian Ocean and the adjacent land regions. However, there is a lack of studies on the isotopic characteristics of rainfall induced by these systems. In this study, we analysed rainwater samples from a few locations in the south and northern coastal regions of the Bay of Bengal during various LPSs and cyclonic events. We found that rainfall isotopes exhibited a large range of variation; intense cyclonic events drove the most depleted values. We hypothesise that isotopic values generated by severe cyclones passed over the sampling site act as outliers. Disregarding such data provides a means to estimate the realistic value of the amount effect. Our results provide new insights into the isotopic behaviour of rainfall during LPSs and cyclones in the northern Indian Ocean, and have implications for paleo-hydroclimate reconstructions using isotopic proxies.

Introduction

The isotopic studies of precipitation provide valuable information on the atmospheric water cycles aimed at understanding the moisture dynamical processes. Several studies describe moisture's origin and transport pathways over the northern Indian Ocean region (Rahul et al., 2016; Sinha et al., 2019). Apart from understanding the moisture dynamical processes, the application of precipitation isotope also extends to past timescales. For example, understanding the causes of past monsoon variability is important because it provides vital clues about how the monsoon will respond to future climate change. Climate scientists often rely on the isotopic analysis of geological deposits, such as the corals and speleothems, to retrieve the past monsoon variability. In terrestrial environments, the speleothems are formed due to the chemical deposition of calcium carbonates in a cave environment. One of the ingredients for speleothem formation is the meteoric water that percolates through the bedrock and enters a cave system. Under certain physiochemical conditions, continuous deposition of mineral layers

forms speleothems. The mineral composition of speleothem is dominantly calcium carbonate (CaCO_3), and its oxygen carries the isotopic signature of rainwater. Hence, the oxygen isotopic values of speleothem essentially provide the isotopic record of rainwater when it was formed. Since the isotopic values of rainwater inversely correlate with the rainfall amount (the amount effect), the isotopic record of speleothem can give a relative estimate of past rainfall variability.

The paleo-monsoon reconstruction using the abovementioned method depends on how well we can establish the amount effect. The amount effect is defined as the relation between the precipitation amount and its isotopic composition, usually weighted average, on a monthly scale. Typically, for every 100mm of rainfall, the isotopic value ($\delta^{18}\text{O}$) decreases by approximately 1.5‰ (Yursev & Gat, 1981). Many people used this value, including in the Indian context (Yadava & Ramesh, 2004). This value, however, varies significantly both spatially and temporally. Chakraborty et al. (2021) examined the spatial variability of the amount effect in India; they observed that the north and the central Indian sites typically show a high amount effect (-4 to -8‰ per 100 mm of rainfall).

On the other hand, the south Indian sites are usually characterised by low values (<-2‰ per 100 mm of rainfall). Though the surface temperature fluctuations create such a north-south gradient, another reason for such variability stems from the statistical artifact. Several investigators quantified the amount effect using only a handful number of samples. With an increase in sample size, the statistical properties between precipitation and its isotopes change, resulting in a different value, albeit a more representative one.

Another reason for this variability arises from the rainfall characteristics. Rainfall shows a large variability, from a few mm to a few hundred mm in a day. Interestingly, the corresponding isotopic values show a much smaller variability. Their statistical distribution characteristics differ significantly (Chakraborty et al., 2020). Heavy to extremely heavy rainfall events produce significantly low isotopic values. Several investigators measured the isotopic values of rainfall during tropical cyclones and observed low isotopic values. It is argued that extreme rainfall events, such as cyclones, are not necessarily part of a monsoon (Singh & Roxy, 2022). Firstly, most cyclones happen during the pre- or post-monsoon seasons. Secondly, a large-scale circulation system causes monsoon rain, while a local to regional scale surface heating causes strong convection resulting in cyclonic storms. When the amount effect is calculated, all kinds of rainfalls (monsoon-induced, cyclonic events, extreme rainfall events, thunderstorm activities) are accounted for to get the monthly rainfall value for a given region. Fousiya et al. (2022) opine that such a practice will likely make the rainfall isotopic data noisy; hence, estimation of the amount effect may incorporate significant error. According to these authors, if the monsoon-induced rainfalls are considered and the anomalous events are disregarded, a better estimation of the amount effect may emerge. This exercise requires characterising the isotopic values of extreme rainfall events. In this study, we characterise the precipitation isotopes of the extreme rainfall events. We use the published isotopic data in India, identify the cyclonic and thunderstorm events, and examine their statistical properties.

Study areas and methodology

The Bay of Bengal is prone to cyclones in the pre-

monsoon (March to May) and post-monsoon (October and November) periods, with some of them occurring during the monsoon (June to September). We analysed the isotopic composition of precipitation from different regions on the Bay of Bengal (BOB) including Port Blair in the Andaman Islands (southern BOB), and a few coastal locations along the northern BOB, such as Kolkata, Barisal, Chittagong, Cox Bazar, and Satkhira. The isotopic data were sourced from Fousiya et al. 2022, Chakraborty et al. 2022, and Tanoue et al. 2018.

The data from Port Blair covers the period from 2012 to 2021, while the data from the northern Bay includes different sites with varying periods ranging from 2010 to 2019. We have chosen oxygen isotopes only since the physical processes affecting hydrogen and oxygen isotopes are nearly identical, resulting in a strong correlation between them.

We have performed the following steps to examine the statistical behaviour of the oxygen isotopic data. We have compiled all the daily data for each region and calculated each dataset's mean and standard deviation (denoted as s). We have generated three subsets of data for each area based on the deviation from the mean: i) the subset that contains only the values within $1s$ of the mean, ii) the subset that contains only the values below $1s$ of the mean, and iii) the subset that contains only the values below $2s$ of the mean. This exercise has also been repeated for the north Bay of Bengal sites.

To calculate the area-averaged (over a grid box of $5\text{-}10^\circ\text{N}$, $80\text{-}95^\circ\text{E}$) monthly value of rainfall, we have used the rainfall data obtained from the Indian Monsoon Data Assimilation and Analysis (IMDAA) project (Rani et al., 2021).

Results and discussion

We calculated the mean and standard deviations of the subsets described in the method section. We plotted the normal distribution curve for each case using these parameters, as shown in Figure 1. The lower panel in this figure shows the southern Bay of Bengal (S-BOB), and the upper panel shows the northern Bay of Bengal (N-BOB). The olive-green plot (a) represents the distribution of all the isotopic values of Port Blair. The purple-brown plot (b) represents the distribution of the values within $1s$ of the mean for this site. The cyan plot (c) represents the distribution of the $\delta^{18}\text{O}$ data with values lower than $1s$ below the mean. The yellow plot (d) represents the distribution of the $\delta^{18}\text{O}$ data with values lower than $2s$ below the mean. The upper panel plots show identical distributions for the north BOB region (e, f, g, h).

The numbers within the distribution curves represent the mean and standard deviation of the precipitation isotopes. The figure also shows how these values change when excluding the values that are less than $1s$ or $2s$ below the mean. These depleted values correspond to the depressions and the cyclonic events that deplete the isotopic composition of rainfall. The mean $\delta^{18}\text{O}$ for the Andaman region is -3.27‰ with a s value of 2.60‰ , and it increases slightly to -2.45‰ when ignoring the values less than mean- $1s$. The distribution subsets comprising the isotope values less than (mean- $1s$) and less than (mean- $2s$) show much lower mean values, -7.74 and -10.53‰ , respectively. It is to be noted that these two subsets represent all kinds of cyclonic events.

The north Bay of Bengal showed similar behaviour. However, its isotopic values were much lower. For example, the average value was -5.47‰ with a variation of 3.85‰ . This was over 2‰ lower than the Andaman region's isotopic mean value. The values also varied widely, from -15 to $+5\text{‰}$ (see Fig. 1e). This is because of the LPSs that are common in this region and cause low isotopic values. Likewise, the extreme values less than (mean - $1s$) and (mean - $2s$) had much lower averages, as shown in Fig. 1g and h.

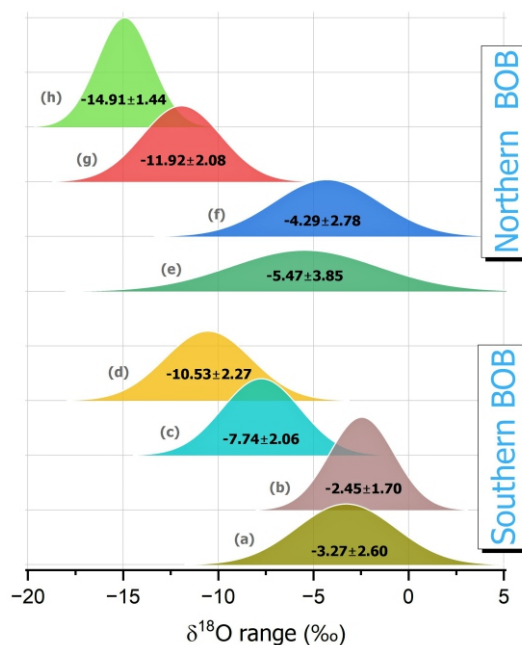


Figure 1. Distribution characteristics of the precipitation isotopes for different data subsets.

To illustrate the precipitation and precipitation-isotope relationship, we need to select a realistic set of isotopic data. This is significant because paleo-monsoon reconstruction involving the isotopic analysis of carbonates, such as speleothems, relies on such a relation. We use monthly correlation analysis between the isotopic and rainfall parameters to estimate the amount effect. We use only the Port Blair data to simplify the calculation because this site has a large dataset

Figure 2 shows the relationship between the monthly rainfall over a $10^\circ \times 10^\circ$ grid box around Port Blair and the monthly precipitation $\delta^{18}\text{O}$. Panel (a) uses the whole $\delta^{18}\text{O}$ dataset. The R^2 value is 0.11 ($p = 0.002$), and the slope is 0.012, meaning an amount effect of -1.2‰ per 100 mm of rainfall. Figure 2b excludes the $\delta^{18}\text{O}$ points that are lower than the mean- 1σ . This process removes most of the low isotopic values caused by depressions, cyclones, etc. This accounts for about 16% of the data. The R^2 value is 0.14 ($p < 0.001$), and the amount effect is -0.6‰ per 100 mm of rainfall. Figure 3b excludes the most depleted values below mean- $2s$ but includes the values between mean and mean- $2s$. R^2 is 0.172 ($p < 0.001$), and the amount effect is -0.9‰ per 100 mm of rainfall. The correlation coefficients in (b) and (c) are slightly higher than in (a). The proportion of data excluded in this case is about 4%. These two parameters, R^2 , and slope (i.e., amount effect) will help us decide which dataset is the most realistic. A high R^2 and slope like 0.015 would be an ideal condition. However, we see that R^2 value is only marginally improved in (b) and (c); also, the slopes are too low compared to the above-mentioned estimate; hence, we need to look for an alternative.

Figure 2a $\delta^{18}\text{O}$ dataset contains one value, November-2013, that acts as an outlier, shown as a red point. Because of the filtering criteria, this value does not appear in the cases of (b) and (c). This outlier was caused by a very severe cyclonic storm Lehar in November 2013. A few other events in this month also produced very low precipitation isotopes. On a monthly scale, this number made the lowest value for the entire observational period of ten years. Hence, we disregard this value as an outlier and regress the remaining $\delta^{18}\text{O}$ values with the rainfall

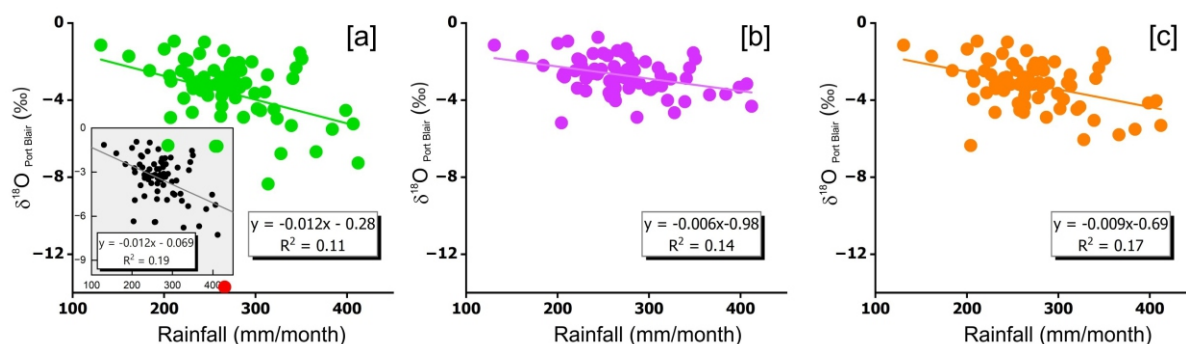


Figure 2. The variations of precipitation and precipitation isotopes on a monthly scale using different data subsets (see the text for the details).

data. The revised analysis is shown in the inset of Figure 2a. We note the R^2 value increases from 0.11 to 0.19 ($p < 0.0001$), while the slope (-0.012) is close to the accepted value of -0.015. So, we observe that removing the most depleted value, only one in the entire dataset yields the maximum correlation coefficient and a reasonable value of the amount effect. However, improving the statistics by a single outlier may not justify altering the result significantly.

The anomalous values produced by the November-2013 cyclonic events may be explained as follows. Several depressions and severe to extremely severe cyclonic storms occurred in the southern parts of the Bay of Bengal in November 2013. Two of them, Phailin and Lehar, were categorised as ESCS (extremely severe cyclonic storms) by the India Meteorological Department. Cyclone Phailin crossed the island (wind speed ~ 75 km/h), about 100 km from Port Blair, causing a nominal isotopic depletion ($\delta^{18}\text{O} \sim -5.5\text{‰}$).

On the other hand, cyclone Lehar passed almost over the sampling site at Port Blair on the 24th and 25th of November with wind speeds over 100 km/h. Due to its proximity to the experiment site, Lehar caused the maximum isotopic depletion ($\delta^{18}\text{O} < -17\text{‰}$). Several other cyclonic events of similar categories were observed in the last ten years. However, none of them produced such low-isotope rainwater because they passed far away from the Port Blair sampling site.

Concluding remarks

This work conveys a vital message. Ignoring the low isotopic values caused by intense cyclonic activities may not enhance the relationship between precipitation and precipitation isotopes. Similarly, improving the correlation value by filtering out only one data point may not be considered statistically rigorous. This dilemma may only be resolved if a robust network of precipitation isotopic sampling strategy is established. The precipitation isotopes varied widely in November-2013 due to significant changes in weather conditions. Taking the temporal average (i.e., monthly mean) reduced that variation considerably, but the mean November-2013 value was still an outlier. The variability could have been lowered further if there was a way to obtain an area-averaged isotopic value. We used the rainfall data over a large region, but such isotopic data is unavailable. Correlating a point source variable with an area-averaged variable likely weakens correlations. This can be improved if area averaging is performed on both variables, potentially yielding a better amount effect value. A precise value of amount effect would help us better quantify the past monsoon variability. Therefore, networking of precipitation isotope measurement is essential to improve the estimation of the amount effect.

References:

- Chakraborty S., Siddharth Birmal, Pramit K. Deb Burman, et al. 2020. Statistical analysis of the precipitation isotope data with reference to the Indian subcontinent. In: Hydrology (Eds) Theodore V. Hromadka II and Prasada Rao; IntechOpen, <http://www.intechopen.com/books/hydrology>.
- Chakraborty, S., Datye, A. et al. 2021 Application of precipitation isotopes in pursuit of paleo-monsoon reconstruction: an Indian perspective, p. 413-427. In: Holocene Climate Change and Environment (eds) Kumaran, N., and Damodaran, P. Elsevier.
- Chakraborty, S., Burman, P.K.D., Sarma, D. et al. Linkage between precipitation isotopes and biosphere-atmosphere interaction observed in northeast India. *npj Clim Atmos Sci* 5, 10 (2022). <https://doi.org/10.1038/s41612-022-00231-z>;
- Fousiya, A.A., Aravind, G.H., Achyutan, H., et al. 2022. Modulation of the precipitation isotopes by the dynamic and thermodynamic variables of the atmosphere in southern parts of India. *Water Resources Research*, 58, e2021WR030855. <https://doi.org/10.1029/2021WR030855>.
- Rahul, P., Ghosh, P. and Bhattacharya, S. K., 2016, "Rainouts over the Arabian Sea and Western Ghats during moisture advection and recycling explain the isotopic composition of Bangalore summer rains", *J. Geophys. Res. Atmos.*, 121, 6148-6163, doi:10.1002/2015JD024579.
- Rani, I., Arulalan T., John P. George, et al. 2021, "IMDAA: High Resolution Satellite-era Reanalysis for the Indian Monsoon Region", *Journal of Climate*, <https://doi.org/10.1175/JCLI-D-20-0412.1>.
- Singh, V. K., & Roxy, M. K. (2022). A review of ocean-atmosphere interactions during tropical cyclones in the north Indian Ocean. *Earth-Science Reviews*, 226, 103967–104023. <https://doi.org/10.1016/j.earscirev.2022.103967>
- Sinha, N., Chakraborty, S., et al. 2019. Isotopic investigation of the moisture transport processes over the Bay of Bengal, *J Hydrol* XV. 2 (doi:10.1016/j.hydroa.2019.100021).
- Tanoue, M., Ichiyangi, K. et al. Seasonal variation in isotopic composition and the origin of precipitation over Bangladesh. *Progress in Earth and Planetary Science* (2018) 5:77
- Yadava, M.G., Ramesh, R. and Pant, G.B. Past monsoon rainfall variations in peninsular India recorded in a 331-year-old speleothem *The Holocene* 14,4 (2004) pp. 517–524.
- Yurtsever, Y. and Gat, J.R. 1981: Atmospheric waters. In Gat, J.R. and Gonfiantini, R. editors, *Stable isotope hydrology: deuterium and oxygen-18 in the water cycle*. Technical Report Series No. 210, Vienna: IAEA, 10342

Research Highlights

Role of atmospheric heat fluxes and ocean advection on decadal (2000–2019) change of sea-ice in the Arctic



A. Mukherjee¹ and M. Ravichandran²

¹ ESSO-National Centre for Polar and Ocean Research (NCPOR), Ministry of Earth Sciences (MoES), Vasco da Gama, Goa, India

² Ministry of Earth Sciences (MoES), New Delhi, India

This article is based on the following paper

Mukherjee, A., Ravichandran, M. Role of atmospheric heat fluxes and ocean advection on decadal (2000–2019) change of sea-ice in the Arctic. *Climate Dynamics* (2022). <https://doi.org/10.1007/s00382-022-06531-7>.

Since 1978, satellite observations have shown that the Arctic sea-ice is declining rapidly compared to the Antarctic and play a major role in global climate variability (Kim et al. 2022). The melting during summer and increased sea surface temperature (SST) are primarily responsible for global weather, climate change, sea-level rise, etc. Process studies related to a decadal reduction of Arctic Sea Ice Concentration (SIC) are an international research interest.

Various studies using reanalysis products and coupled sea-ice models showed possible dynamics and thermodynamics associated with the rapid Arctic sea-ice decline. Recent studies show a decreasing trend of Arctic summer sea-ice since 2000 (Swart et al. 2015), with record minimum sea-ice extent during 2012 (Parkinson and Comiso 2013). This highlights the importance of a study related to the recent decadal change (decade between 2010–2019 and 2000–2009) of Arctic SIC and SST using satellite observations and a numerical model. No systematic studies have been carried out on the significance of net atmospheric heat flux and ocean advection on recent decadal (2000–2019) changes in Arctic sea-ice and SST using heat budget analysis. Our study shows the contribution of oceanic advection and net atmospheric heat fluxes on recent decadal changes of SST and SIC using heat budget analysis from a global ocean sea-ice coupled model for the eight sectors of the Arctic.

Global ocean sea-ice coupled model

As a part of polar sea-ice related studies at the National Centre for Polar and Ocean Research (NCPOR), Ministry of Earth Sciences (MoES), we developed a global ocean sea-ice coupled model combining the Modular Ocean Model (MOM) version 5 and ice model Sea ice simulator (SIS) hereafter referred as MOMSIS. The horizontal resolution of the model is set to $0.25^\circ \times 0.25^\circ$ globally. The model has 50 vertical levels with a 10 m resolution from the surface to 220 m. The model uses the tripolar grid with poles over Eurasia, North America, and Antarctica to avoid polar filtering Arctic (Murray 1996). Sea surface salinity is relaxed to

the monthly global climatology of Chatterjee et al. (2012) with 60 days time scale to implicitly include the impact of river runoff forcing in the MOMSIS.

MOMSIS starts with the global temperature and salinity climatology of Chatterjee et al. (2012) during January. The model is forced with CORE-II atmospheric forcing (Large and Yeager 2008) of air pressure, downward and longwave radiation, air temperature, specific humidity, precipitation, and snowfall at 2m, and wind stress at 10 m with a horizontal resolution of $2^\circ \times 2^\circ$. After 100 years of climatological spin-up, MOMSIS starts with real-time atmospheric forcing from January 1979 using ECMWF ERA5 (Wang et al. 2019) with a horizontal resolution of $0.25^\circ \times 0.25^\circ$ and a temporal resolution of 6 hours. This study analysed model outputs from January 2000 to December 2019 for the decadal change of SIC and SST in the Arctic Ocean.

Validation

The Arctic region between 0° E– 360° E and 60° N– 90° N has been divided into eight sectors; five in the east and three in the west. The eight sectors named S01, S02, S03, S04, S05, S06, S07, and S08 include the major part of the Norwegian, Barents, Kara, Laptev, East Siberian, Chukchi, Beaufort, and Greenland Seas, respectively. Details of the above Arctic sector regions are shown in Fig. 1.

The performance of the MOMSIS is slightly better in the simulation of satellite-derived Advanced High Resolution Radiometer (AVHRR) observed SST compared to SIC in almost every sector. Higher correlation (R) values have been observed for SST in the Norwegian (part of S01) and Greenland (part of S08) Sea regions of the Arctic compared to SIC (Fig. 1). Also, a root mean percentage error (RMPE) for SIC and SST has been estimated with low RMPE (less than 40 %) at almost every sector of the Arctic except few locations (Fig. 1).

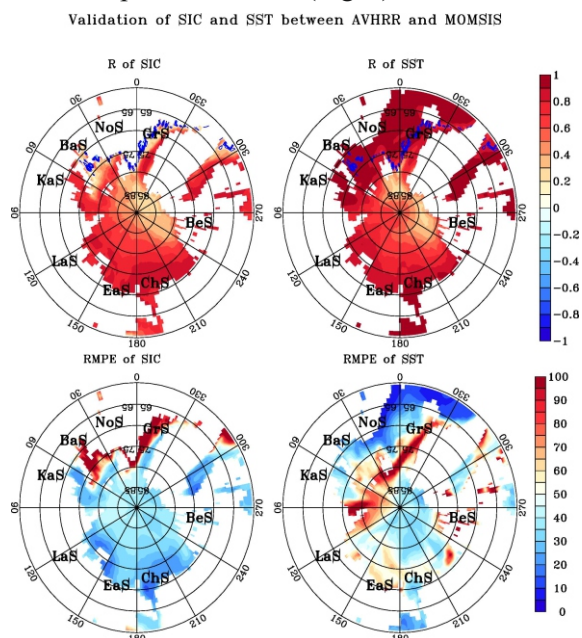


Fig. 1: The left panel of the figure shows the correlation (R, top) and root mean percentage error (RMPE, bottom) between AVHRR observed Sea ice concentration (SIC) and model MOMSIS. The right panel of the figure shows R (top) and RMPE (bottom) for Sea surface temperature (SST). Time series daily data from 01 January 2000 to 31 December 2019 has been used to estimate R and RMPE values in the Arctic regions. R values within the blue contour (-0.1 to 0.1) imply a statistical significance of less than 90 %. Eight major seas written in bold font imply the dominance of above sea for that region. In the figure, NoS, BaS, KaS, LaS, EaS, ChS, BeS, and GrS represent the Norwegian, Barents, Kara, Laptev, East Siberian, Chukchi, Beaufort, and Greenland Seas, respectively.

Observed and simulated decadal change of SIC and SST in the Arctic.

AVHRR data shows a similar maximum decadal reduction of SIC during the summer and autumn seasons in the Barents (part of S02), Kara (part of S03) and Laptev (part of S04) Sea regions of the Arctic as observed during other seasons (Fig. 2). MOMSIS also shows similar maximum decadal reduction of SIC in all above three regions of the Arctic during summer and autumn seasons. As in AVHRR observations, MOMSIS also successfully simulates very small decadal changes of SIC in the western Arctic regions, including Beaufort (part of S07) and Chukchi (part of S06) Sea regions during all four seasons. However, MOMSIS shows a very small decadal decrease of SIC in the Greenland Sea during all four seasons (Fig. 2). AVHRR showed statistical significance for decadal change at 06 sectors except Chukchi (part of S06) and Beaufort (part of S07) Seas. However, MOMSIS showed 90 % statistical significance in all eight sectors of the Arctic.

Decadal change of SIC

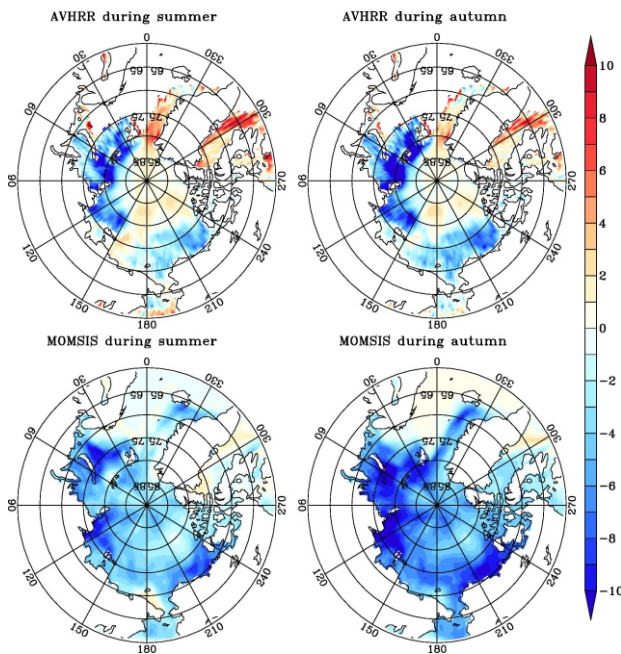


Fig. 2: Comparison of decadal change of SIC (in %) in the Arctic between AVHRR and MOMSIS during summer (left panels) and autumn seasons (right panels). Decadal change is estimated by subtracting decadal climatology between 2010–2019 and 2000–2009.

Upper ocean heat budget analysis for the decadal change

Upper ocean mixed layer depth (MLD) heat budget analysis has been performed to understand the role of Net Atmospheric Heat (NAH) flux and ocean advection on the decadal change of SST and SIC. In the heat budget, rate of mixed layer temperature rate is balanced by net atmospheric heat flux, ocean advection and residual processes which includes vertical entrainment, ocean mixing, internal instability etc. Using MLD heat budget analysis (Vialard and Delecluse 1998), it has been observed that decadal change of NAH flux plays the most significant role in the maximum decadal decrease of SIC and increase of SST during all four seasons in the Arctic. It was more than 90 % statistically significant at Kara (part of S03), Laptev (part of S04), East Siberian (part of S5), and Beaufort (part of S07) Sea regions (Fig. 3). Maximum average decadal increase of NAH flux has

been observed in the Barents (part of S02), Kara (part of S03) and Laptev (part of S04) Sea regions of the Arctic during summer seasons and was responsible for the decadal increase of mixed layer temperature (MLT) rate and also, an increase of average SST in above regions.

It has been observed from the MLD heat budget analysis that destructive interference between the decadal change of NAH fluxes and ocean advection plays the most crucial role in the very small decadal decrease of SIC and increase of SST in the Norwegian (part of S01) and Beaufort (part of S07) Sea regions of the Arctic. At the Norwegian Sea (part of S01), only decadal change of ocean advection is 90 % statistical significance. However, at Beaufort (part of S07) Sea, both NAH fluxes and ocean advection are at a 90 % statistical significance level.

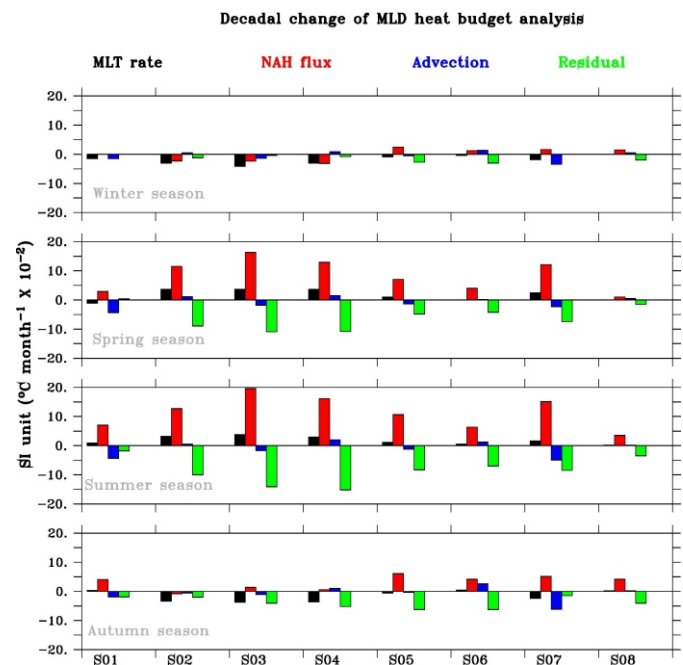


Fig. 3: Histogram showing the decadal change of Mixed Layer Depth (MLD) heat budget analysis in the Arctic. Each box's black, red, blue, and green colour values represent the Mixed Layer Temperature (MLT) rate, net atmospheric heat (NAH) flux, ocean advection, and residual processes, respectively. Four panels in the figure represent heat budget analysis for four seasons; winter, spring, summer and autumn. Here, in the X-axis, a total of eight sectors named S01, S02, S03, S04, S05, S06, S07, and S08 represent a major part of the Norwegian, Barents, Kara, Laptev, East Siberian, Chukchi, Beaufort, and Greenland Seas, respectively. The Y-axis represents the unit of all four heat budget terms in the SI unit ($^{\circ}\text{C}/\text{month}$).

Upper ocean heat budget analysis for the decadal change

It is known from earlier research that Norwegian (part of S01) Sea regions are the major pathways for the intrusion of warmer Atlantic water in the Arctic (Kim and Kim, 2019; Wang et al., 2020). Similarly, Beaufort (part of S02) Sea regions are the major pathways for the intrusion of warmer Pacific water in the Arctic (Armitage et al., 2020). Using MLD heat budget analysis, a similar decadal solid change of ocean advection has been observed in the Norwegian (part of S01) and Beaufort (part of S02) Sea regions of the Arctic during all four seasons. The substantial decadal decrease of ocean advection in the above two sectors plays an important role in the slight decrease of SIC and increase of SST in the above two sectors compared to other sectors in the Arctic during all four seasons.

MOMIS also shows that spatial variations strongly dominate decadal changes in ocean advection. Similar spatial variations were also observed for decadal change of NAH fluxes. Also, horizontal ocean advection dominates compared to vertical ocean advection contribution for decadal change of SIC and SST. Very small and negligible decadal vertical advection shift has been observed along all eight sectors of the Arctic during all four seasons.

The study results are restricted to the decadal variability of SIC and SST during four seasons in the Arctic and the possible role of decadal change of atmospheric net heat fluxes and ocean advection on it. Detailed studies related to decadal change of possible pathways of ocean advection and inclusion of warmer Atlantic and Pacific water in the Arctic need to be investigated.

References

- Amritage TWK, Manucharyan GE, Petty AA, Kwok R, Thompson AF (2020) Enhanced eddy activity in the Beaufort Gyre in response to sea ice loss. *Nat Commun* 11:761. <https://doi.org/10.1038/s41467-020-14449-z>
- Chatterjee A, Shankar D, Shenoi SSC, Reddy GV, Michael GS, Ravichandran M, Gopalkrishna VV, Rao EPR, Bhaskar TVSU, Sanjeevan VN (2012) A new atlas for temperature and salinity for north Indian Ocean. *J Earth Syst Sci* 121:559–593. <https://doi.org/10.1007/s12040-012-0191-9>.
- Kim J, Kim K (2019) Relative role of horizontal and vertical processes in the physical mechanism of wintertime Arctic amplification. *Clim Dyn* 52:6097–6107. <https://doi.org/10.1007/s00382-018-4499-2>.
- Kim J, Kug J, Hoon J, Zeng N, Hong J, Jeong J, Zhao Y, Chen X, Williams M, Ichii K, Strub G (2022) Arctic warming-induced cold damage to East Asian terrestrial ecosystems. *Commun Earth Environ*. <https://doi.org/10.1038/s43247-022-00343-7>.
- Large WG, Yeager SG (2008) The global climatology of an interannually varying air–sea fluxdata set. *Clim Dyn* 33:341–364. <https://doi.org/10.1007/s00382-008-0441-3>.
- Murray RJ (1996) Explicit generation of orthogonal grids for ocean models. *J Comput Phys* 126:251–273. <https://doi.org/10.1006/jcph.1996.0136>.
- Parkinson CL, Comiso JC (2013) On the 2012 record low Arctic sea ice cover: combined impact of preconditioning and an August storm. *Geophys Res Lett* 40:1356–1361. <https://doi.org/10.1002/grl.50349>.
- Swart NC, Fyfe JC, Hawkins E, Kay JE, Jahn A (2015) Influence of internal variability on Arctic sea-ice trends. *Nat Clim Change* 5:86–89. <https://doi.org/10.1038/nclimate2483>.
- Vialard J, Delecluse P (1998) An OGCM study for the TOGA decade. Part I: role of salinity in the physics of the western Pacific fresh pool. *J Phys Oceanogr* 28:1071–1088. [https://doi.org/10.1175/1520-0485\(1998\)028<1071:AOSFTT>2.0.CO;2](https://doi.org/10.1175/1520-0485(1998)028<1071:AOSFTT>2.0.CO;2)
- Wang C, Graham RM, Wang K, Gerland S, Granskog MA (2019) Comparison of ERA5 and ERA-Interim near-surface air temperature, snowfall and precipitation over Arctic sea ice: effects on sea ice thermodynamics and evolution. *Cryosphere* 13:1661–1679. <https://doi.org/10.5194/tc-13-1661-2019>
- Wang Q, Wekerle C, Wang X, Danlov S, Koldunov N, Sein D, Sldorenko D, Appen W, Jung T (2020) Intensification of the Atlantic water supply to the Arctic ocean through Fram Strait induced by Arctic sea ice decline. *Geophys Res Lett* 47:e2019GL086682. <https://doi.org/10.1029/2019GL086682>.

Research Highlights

Wave induced coastal flooding along the southwest coast of India during tropical cyclone Tauktae



Ratheesh Ramakrishnan¹, Remya P G², Anup Mandal¹, Prakash Mohanty², Prince Aryakandy³, Mahendra R S², Balakrishnan Nair²
¹Space Applications Centre (SAC), ISRO, Ahmedabad
²Indian National Centre for Ocean Information Services (INCOIS), Hyderabad
³Fisheries Engineering, Kerala University of Fisheries and Ocean Studies (KUFOS), Kerala

This article is based on the following paper:

R Ratheesh, PG Remya, A Mandal, P Mohanty, P Arayakandy, et al (2022). Wave induced coastal flooding along the southwest coast of India during tropical cyclone Tauktae, *Scientific Reports* 12 (1), 19966

The coastal areas worldwide is adversely impacted by the climate change, in which the increase in tropical cyclones and its intensity have marked a significant concern among the coastal community. The Northern Indian Ocean is one of the world's cyclone prone area (Sahoo and Bhaskaran, 2018). Arabian Sea, in recent past have witnessed more intense cyclones, where 150% increase in the cyclone is reported during last two decades, making the western Indian coast vulnerable to threats like storm surge and high waves. The Tauktae cyclone formed in Arabian Sea on May 14, 2021, moved northwards as it intensified into VSCS. The coast of Kerala, especially along the Chellanam coast, in the district of Ernakulam, Kerala witnessed severe coastal flooding that damaged the coastal dwellings and infrastructure. The storm surge predicted with the operational forecast system was marginal at the Chellanam coast and showed no coastal inundation; moreover, the wave impact at the Chellanam coast corresponded with the low tide time. Despite these unfavourable conditions, the coast was severely flooded with wave overwash.

When high waves approach the coastal region, associated wave properties can significantly affect the wave run up elevation depending on the bathymetric condition. We used XBeach (Roelvink et al., 2018) numerical model to investigate the complex coastal wave dynamics at Chellanam region due to the Tauktae cyclone. A coastal high-resolution blended bathymetry and topography database was prepared for this study. The bathymetry data is a blend of in-situ data (hydrographic charts, surveyed data from ships) for coastal regions. The XBeach model is configured in 2D, where we have considered 20 m bathymetry contour as the offshore boundary. The wave spectrum extracted from the operational WAVEWATCH III at the offshore boundary of the coastal domain is used as the open boundary condition for the 2D XBeach model.

We observed the influence of infragravity (IG) waves that are associated with incoming short waves (Bertin et al., 2018). The infragravity waves increase the run up elevation. The wave height of the IG waves increases from negligible height at the boundary toward the coast. Figure 1 shows the cross-shore change in the significant wave height of short wave and IG waves for two regions A and B located to the north and south of the domain

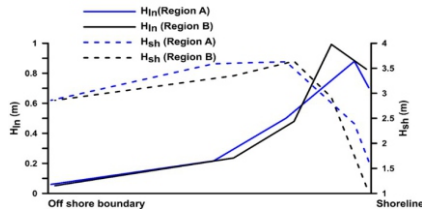


Figure 1. The change in the significant wave height of IG waves and short waves from offshore boundary to the shoreline.

respectively. IG waves peaks at about 5 m depth and gradually decreases to the shoreline. The Chellanam coast experienced IG waves of about 0.8 to 1 m height during the Tauktae cyclone. As the infra gravity waves increase the coastal surface water elevation, they significantly contribute towards extending the coastal inundation during the wave over wash under cyclone conditions.

The coastal water elevations are also increased due to the wave setup formed under breaking waves, where the cross-shore gradient in the radiation stress results in the rise of the mean water level at the coast (Wu et al, 2018). The water level corresponding to peak storm is analyzed to obtain the maximum water level at each grid and is shown in figure 2. The water level near the coast have reached to a maximum of about 0.7 due to the wave setup. The effect of IG waves and the rise in the coastal water level due to wave setup caused the inundation at Chellanam, even during low tide with negligible surge height. The study emphasizes the importance of longwave and wave setup and its interaction with nearshore bathymetry during the high wave.

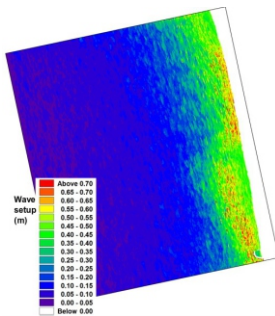


Figure 2. Simulated maximum wave set up during the period of TC Tauktae at Chellanam

References

- Bertin, X., et al. Infragravity waver: From driving mechanisms to impacts. *Earth-Science Reviews*, 177, 774-799 (2018)
- Roelvink, D., McCall, R., Mehvar, S., Nederhoff, K. and Dastgheib, A. Improving predictions of swash dynamics in XBeach: The role of groupiness and incident-band runup. *Coastal Engineering*, 134, 103-123 (2018)
- Sahoo, B. and Bhaskaran P.K. A comprehensive data set for tropical cyclone storm surge-induced inundation for the east coast of India. *International Journal of Climatology*, 38, 403-419(2018)
- Wu G., Shi F., Kirby J.T., Liang B and Shi J (2018) Modeling wave effects on storm surge and coastal inundation. *Coastal Engineering*, 140, 371-382 (2018)

Publication committee

Dr Sanil Kumar Dr Ananth Parekh Dr Pattabhi Ramarao Dr Tune Usha Ms Divya David Prof Vimlesh Pant Dr Smitha Balraj
Editorial board members: Dr M. Baba Dr JayaKumar S Dr R Venkatesan Dr M Sudhakar Dr Siby Kurian Dr Sanil Kumar
 Dr Lidita Khandeparkar Dr Pratima Kessarkar Dr K J Ramesh

Design/Typset/Editing: Kirti Dubhashi

Cover Photo: The image shows a mesocosm experiment conducted in the open Arabian Sea during the spring inter-monsoon (April) of 2022 by CSIR NIO. The experiment in mesocosm bags uses natural buoyant flakes made out of rice husk and iron ore reject, which will provide the required nutrients to increase biological production and sequester atmospheric CO₂. The present experiment is the first in the series of experiments needed to check the efficacy of the buoyant flakes before venturing for open ocean trials. **Image courtesies:** Dr. Damodar M. Shenoy, Scientist, CSIR -National Institute of Oceanography, Dona Paula, Goa

OSI Webinar Series(January-March 2023)

Topic: Coastal Management Information System for South Indian Coastal States

Speaker: Dr.Sriganesh Jeyagopal, Principal Scientist, National Centre for Ports, Waterways and Coasts, IIT Madras.



Date&Time: 05 January, 2023 (Thursday), 1600-1700 IST

About the Talk: Coasts are exposed to hazards that are natural (global warming-induced sea-level-rise, river mouth closure by siltation, changing climate with the increased frequency of cyclonic storm surge, coastal flooding, tsunami, etc.) and due to anthropogenic activities (shoreline erosion, dredging, sewage treatment plants, desalination plants, etc.). There are several proven site specific hard/soft/hybrid engineering coastal protections that are in practice for a hazard around the world and different advanced techniques available to defend and preserve the coasts from hazards. Apart from combating the hazards, there is rapid progress in coastal development (on/offshore). There is an insufficient information and/or limited historical records on the physical met-ocean parameters responsible for the stability of the shore/coasts. This talk on Coastal Management Information System (CMIS) focuses on the physical field data collections on Tide, Wave, Current, Beach Profile, Shoreline, near shore & seabed Sediments characteristics for Coastal Protections, Planning, Design of Mitigation Structures, schemes for Sustainable Coastal Conservation & Developments.

Topic: Application of precipitation isotopes in studying the monsoon processes

Speaker: Dr. Supriyo Chakraborty, Visiting Faculty, Savitribai Phule Pune University, Pune



Date&Time: 14 March, 2023 (Tuesday), 1600-1700 IST

About the Talk: Isotopic analysis of precipitation investigates the hydrological problems and moisture dynamics. In the Indian context, the hydrological characteristics are intricately linked to the monsoon processes. Hence, it is essential to understand how the precipitation isotopes are controlled by the monsoon rainfall and its associated variables. In this talk, Talk discussed how the precipitation isotopes observed at an island in the Bay of Bengal responded to the monsoon system and, in turn, how we could use them to understand the past monsoon variability better.

Articles/research highlights of general interest to the oceanographic community are invited for the next issue of the Ocean Digest. Contributions may be emailed to osioceandigest@gmail.com